Biointerface Research in Applied Chemistry
Open-Access Journal (ISSN: 2069-5837)

Article
Volume 13, Issue 2, 2023, 200
https://doi.org/10.33263/BRIAC132.200

Hemigraphis colorata (HC) Leaves Extract as Effectual Green Inhibitor for Mild Steel Corrosion in 1M HCl

Supriya Bangera [1], Vijaya D.P. Alva [1], Pavithra Neriyana Sannaiah [1]

[1] Department of Chemistry, Shree Devi Institute of Technology, Kenjar, Mangalore, Karnataka, India
* Correspondence: alvavijaya@gmail.com (V.D.P.A);

Scopus Author ID 54398258500
Received: 3.01.2022; Accepted: 13.02.2022; Published: 7.04.2022

Abstract: The corrosion inhibitory effect of *Hemigraphis colorata* (HC) leaves extract on mild steel in 1M HCl was investigated using mass loss measurements, ultraviolet-visible(UV) spectroscopy, Fourier transform infrared spectroscopy(FT-IR), electrochemical impedance spectroscopy (EIS), and Tafel polarization techniques at the temperature range of 303K-323K. The optimum inhibition efficiency of HC extract at 303K, 313K, and 323K was found to be 90.2%,92.77%, and 93.73%, respectively, for the maximum concentration of the extract. This suggests that inhibition efficiency was found to increase with increasing concentration of the leaves extract at all the temperatures and increasing solution temperature. The adsorption process complied with a Langmuir adsorption isotherm. Polarization measurements suggest a mixed mode of corrosion inhibition. The activation energy and other thermodynamic parameters were calculated for the process of inhibition. The adsorbed invisible layer was investigated using scanning electron microscopy, which revealed better morphology of mild steel in extract presence. Using energy-dispersive X-ray spectroscopy, the effect of HC extract on the interfacial behavior of mild steel surface was analyzed.

Keywords: *Hemigraphis colorata*; mild steel; adsorption.

1. Introduction

Metals are highly prone to corrosion, which has been a significant problem facing since the start of the industrial revolution. Corrosion can occur in various systems, including cooling systems, oil production units, oil storage tanks, pipeline protection, refinery units, etc. Corrosion causes damage to infrastructure and machines, which are usually expensive to repair, costly in terms of loss due to contaminated products, loss in terms of environmental damage, and possibly costly in terms of human safety. Corrosion is threatening the stability of the industry's, putting employees and the environment's safety at danger. Corrosion is a mechanism that involves a chemical or electrochemical reaction between materials, usually metal, and their environment that produces a deterioration of the materials and their properties [1]. Material damage can be prevented by using various approaches such as upgrading materials, blending of production fluids, coating, process control, and chemical inhibition. Among these methods, corrosion inhibitors are one of the most appropriate, effective, and economical ways of mitigating corrosion problems in corrosive media [2]. Corrosion inhibitors are substances that, upon addition to a corrosive environment, reduce corrosion rate to an acceptable level [3]. Several synthetic corrosion inhibitors have been successfully used to control the corrosion of metals and alloys in various media. Large numbers of organic compounds having hetero atoms,

conjugated π-bonds, and aromatic nuclei acted as promising inhibitors [4-6]. However, most synthetic inhibitors are toxic, expensive, and hazardous to the environment. Hence health and safety are major concerns when selecting corrosion inhibitors. This has prompted researchers to find green alternatives that are non-toxic, biodegradable, cheap, and efficient [7, 8]. Thus, corrosion inhibition is geared towards creating environmentally safe corrosion inhibitors that offer high inhibition efficiency without a detrimental effect on the environment. Plant extract is low-cost and environmentally safe, so the main advantage of using plant extracts as corrosion inhibitors is that it is economical and safe for the environment. The inhibition potential of plant extract is usually associated with the existence of phytochemical constituents. These constituents often possess polar functionalities with heteroatom as well as triple or conjugated double bonds or aromatic rings in their molecular structures, which serve as the primary adsorption sites [9, 10]. Due to the high technological value of metals and alloys and the wide range of applications it has, corrosion protection of metals and alloy has been a topic of research for a long time. The literature study reveals several publications that describe the inhibitory effects of several plant extracts on metals and alloys. Several plant leaf extracts have been tested for their corrosion inhibition properties in acid media, including *Cerumium rubrum, Euphorbia heterophylla, Gongronema latifoliuim, Ochrosia oppositifolia* and isoreserpiline, *Piper longum, Murraya koenigii, Phyllanthus amarus, Azadirachta indica* [11-18]. The purpose of the study is intended to find an effective alternative for conventional and hazardous corrosion inhibitors. Hence, the current investigation selected a novel environmentally friendly Hemigraphis Colorata (HC) leaf as an effective corrosion inhibitor. HC, commonly known as a metal leaf, is a perennial herb chiefly grown as an ornamental plant belonging to the family Acanthaceae, native to the eastern Malesia region, cultivated in India [19]. In south India, the plant is known as Murikooti or Murianpacha due to its incredible potency to heal wounds. It is claimed in folk medicines for various skin diseases; the leaves are ground into a paste and applied on fresh-cut wounds to promote wound healing and used to treat anemia [20-22]. The plant was known for its anti-inflammatory properties, antioxidant, anti-diabetic, and antibacterial activity [23]. The current study investigates the anticorrosive properties of HC leaves extract in 1 M HCl solution on mild steel corrosion.

2. Materials and Methods

2.1. Preparation of coupon.

The mild steel specimens employed in the present work with composition 0.18 % C, 0.6 % Mn, 0.04% P, 0.05% S, 0.1 % Si, and balance Fe was used for mass loss and electrochemical studies. For mass loss, mild rectangular steel measuring 3x1.5x0.3cm was used, while mild steel specimens embedded in epoxy resin with an exposed surface area of 1 cm^2 were used for polarisation and EIS measurement as working electrodes. Before beginning the trials, the mild steel pieces were thoroughly wiped with various grades of emery paper (grade 100-2000) to remove adhering impurities. It was then washed with deionized water, then cleaned with acetone, and dried at ambient conditions before dipping it into the acid solution.

2.2. Preparation of corrosive solution.

Diluting laboratory-grade 37 % HCl with distilled water to yield 1 M corrosive HCl solution. In each experiment, the concentration of the extract used was 0.1-1.0 g/L, the leaf

extract was readily soluble in the corrosive medium, and the volume of the corrosive solution utilized was 50 ml.

2.3. Inhibitor.

The fresh leaves from HC were congregated from a single tree, washed under tap water and then with deionized water, cut into tiny parts, dried under sunlight for 4 days, and then acquired dried leaves were ground into a powder with pestles and mortars. In the Soxhlet apparatus, about 100 g of HC leaf powder was wrapped uniformly and placed in a thimble. Next, the colorants of the leaves were extracted with 500 mL of distilled water for 6 hours at 60°C. After complete extraction, the extract was filtered; the solvent was evaporated and then dried to obtain solid mass. Typical leaves of the HC plant are shown in Figure 1.

Figure 1. Typical leaves of a HC plant.

2.4. Mass loss measurements.

Mild steel specimens that were polished and dried with dimensions of 3x1.5x0.3 cm were weighed using a digital balance with a sensitivity of 1mg. After weighing precisely, the mild steels were dipped in 1 M HCl for 24 hours at 303K in the absence and presence of various concentrations of extract such as 100, 200, 500, and 1000ppm. After 24 hours, the inhibited/corroded metals were drawn out from an acid medium, rinsed thoroughly with deionized water, hot air dried, stored in a desiccator, and reweighed. For the calculations of inhibition efficiency on a percentage scale, triplicate studies were performed, and the average mass loss value was determined. in the absence and presence of various concentrations such as 100, 200, 500 and 1000ppm

2.5. Electrochemical measurements.

Electrochemical testing was performed in a three-electrode cell using Gill AC 1864 of an ACM electrochemical workstation connected with a personal computer. The electrochemical cell is comprised of three-electrode configuration with a mild steel specimen as a working electrode (WE), a platinum electrode as an auxiliary electrode (AE), and a saturated calomel electrode (SCE) as the reference electrode (RE). Each run was carried out in aerated solutions at the required temperature, using a thermostatically controlled water bath under stagnant conditions. Under the stagnant condition, corrosion product scale can easily form, which is believed to play an important role in the corrosion inhibition mechanism and kinetics. The mild steel was immersed in the test solution for 5-10 minutes until the open circuit potential E was reached. The potentiodynamic current–potential curves were executed at a scan

rate of 1mV sec^{-1}, and the potential was started from -250mV to +250mV versus open circuit potential at different temperatures (303K, 313K & 323K). We carried out EIS measurements at the open circuit potential between the frequency ranges of 100 kHz and 0.01 Hz using a small amplitude of 10 mV AC signals at 303K and analyzing the impedance data with a Nyquist plot. For the calculations of percentage inhibition efficiency, triplicate studies were performed, and the best inhibition efficiency was reported.

2.6. Surface scrutiny.

To investigate the influence of the phytochemical constituent of the extract on the corrosion phenomenon of mild steel, the photographs of fresh inhibited and uninhibited mild steel samples were recorded using SEM-EDXS. Using CARL ZEISS sigma Field Emission scanning electron microscopes, the morphology of steel samples was analyzed. The mild steel specimens were immersed for 24 hours in 1M HCl solution without and with 1000 ppm of HC leaves extract at 303K. After 24 hours, the mild steel was taken out of the test solution, rinsed with di ionized water, dried, and submitted for SEM and EDX.

2.7. Extract characterization.

2.7.1. Infrared spectroscopy characterization.

Infrared Spectrophotometer-based methods are perhaps the most effective technique for detecting functional groups in various compounds. FTIR spectra of the HC extract were recorded using the same instrument was discussed in our prior paper [62]. In addition to the HC extract, the protective layer of HC extract scraped from the metal surface after corrosion was tested by loading the sample into an FTIR spectrometer at room temperature. FTIR peaks were recorded for scans within the wavelength range 4000-400 cm^{-1}.

2.7.2. UV-Visible technique.

The UV-visible spectra were recorded using a Shimadzu UV-1800 spectrophotometer with a wavelength limited between 500 and 150 nm to assess the adsorption of HC extract constituents on a mild steel surface in 1 M HCl. The spectra were obtained for 1 M HCl solution containing 1000 ppm of the extract with and without mild steel sample immersed for 24 hours.

3. Results and Discussion

3.1. Mass loss measurements.

The acquired corrosion parameters by performing mass loss measurements for mild steel without and with various concentrations of HC leave extract in 1M HCl at 303K are tabularized in Table 1. The percentage inhibition efficiency η (%) was calculated using the relationship [24]

$$\eta\,(\%) = \frac{w_1 - w_2}{w_1} \times 100 \qquad (1)$$

where w_1 and w_2 are the mass loss values without and with the different concentrations of the HC inhibitor, respectively. From Table 1, it was seen that amount of mass loss is found to decrease with increasing the extract concentration, i.e., the inhibition efficiency increased with the inhibitor concentrations.

Table 1. Corrosion parameter calculated through mass loss in 1M HCl solution for mild steel with and without various concentrations of HC leaves extract.

Inhibitor Concentration (ppm)	Loss of mass (g)	η (%)	Standard Deviation
Blank	1.2431	--	1.8%
100	0.9924	20.1	2.1%
200	0.5412	56.2	1.9%
500	0.4790	61.4	1.9%
1000	0.1721	85.1	2.7%

3.2. Electrochemical measurements.

3.2.1. Open circuit potential (OCP).

The open-circuit potential time curves for mild steel in solution in the absence and presence of different concentrations HC leaf extract is shown in Figure 2. Before electrochemical impedance spectroscopy and potentiodynamic polarization measurements, the working electrode should first be stabilized by immersion in the test solution for 30 minutes. Compared to the blank condition, the open potential shifted positively in the solutions containing inhibitor, which could be explained by the adsorption of HC leaf extract on the mild steel surface[25]. Hence, the maximum OCP difference between the blank and HC extract is 51 mV. As a result, it can be said that the extract works as a mixed-type corrosion inhibitor [29].

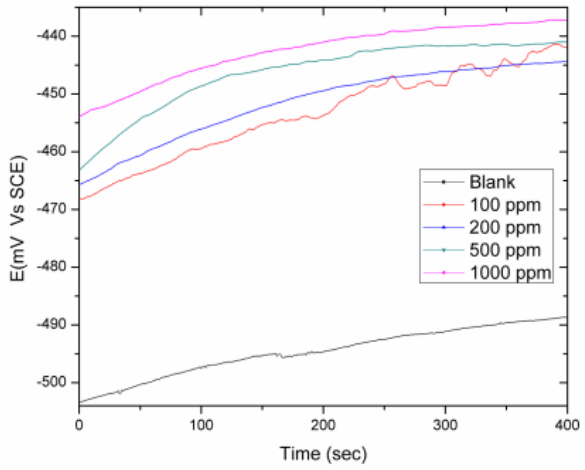

Figure 2. Open circuit potential-time curves for mild steel in 1M HCl solution with various HC leaf extract concentrations.

3.2.2. Potentiodynamic polarization measurements(PDP).

The consequence of varied concentrations of HC inhibitor on the anodic and cathodic activity of mild steel in 1M HCl at 303K, 313K & 323K was studied, and the resulting Tafel curves are shown in figures 3(a), 3(b) and 3(c) respectively. Electrochemical parameters derived from these curves, such as corrosion current density (I_{corr}), corrosion potential (E_{corr}), and Tafel slopes (β_a and β_c) are described in Table 2. The percentage inhibition efficiency (η (%)) of leaves extract was calculated using the relationship given below [26], and their data are mentioned in Table 2.

$$\eta\,(\%) = \frac{I_{corr} - I^{*}_{corr}}{I_{corr}} \times 100 \qquad (2)$$

where I_{corr} and I^{*}_{corr} are the corrosion current in the absence and in the presence of the inhibitor, respectively.

The corrosion rate (ν_{Corr}) is evaluated by the expression [27]

$$\nu_{Corr} = \frac{k \times M \times I_{corr}}{Q \times Z} \quad (3)$$

where k is a constant that defines corrosion rate, I_{corr} the corrosion current in cm^{-2}, Z number of electrons transferred per metal atom, M atomic mass of the metal, and Q density of the corroding materials. Results presented in Table 2 show that the extract serves as a good corrosion inhibitor for mild steel in 1 M HCl solution, as the corrosion rate of the metal decreased with an increase in inhibitor molecule concentration at all of the studied temperatures. With an increase in the concentration and temperature, the inhibition efficiency of HC leaves extract increases. Due to the physisorption of HC molecule adsorbed at low temperature on the mild steel surface and shifted to chemisorptions at higher temperature [28]. Figure 4 shows the effect of temperature on the inhibition efficiency at varying extract concentrations. The available data from Table 2 also shows that I_{corr} was decreased with the addition of HC leaves extract at all of the tested temperatures, and it continuously decreased with increasing inhibitor concentration. The inhibitive ability, which is reflected by η(%), markedly improved as the inhibitor concentration increased. Meanwhile, an inhibitor can be classified as an anodic- or cathodic type when the difference in the E_{corr} values of blank and inhibitor is larger than ± 85 mV [29]. But in the present study, the largest displacement exhibited by the extract was 74 mV vs. SCE, which indicated a mixed-mode of inhibition by inhibiting both hydrogen evolution and mild steel dissolution reaction.

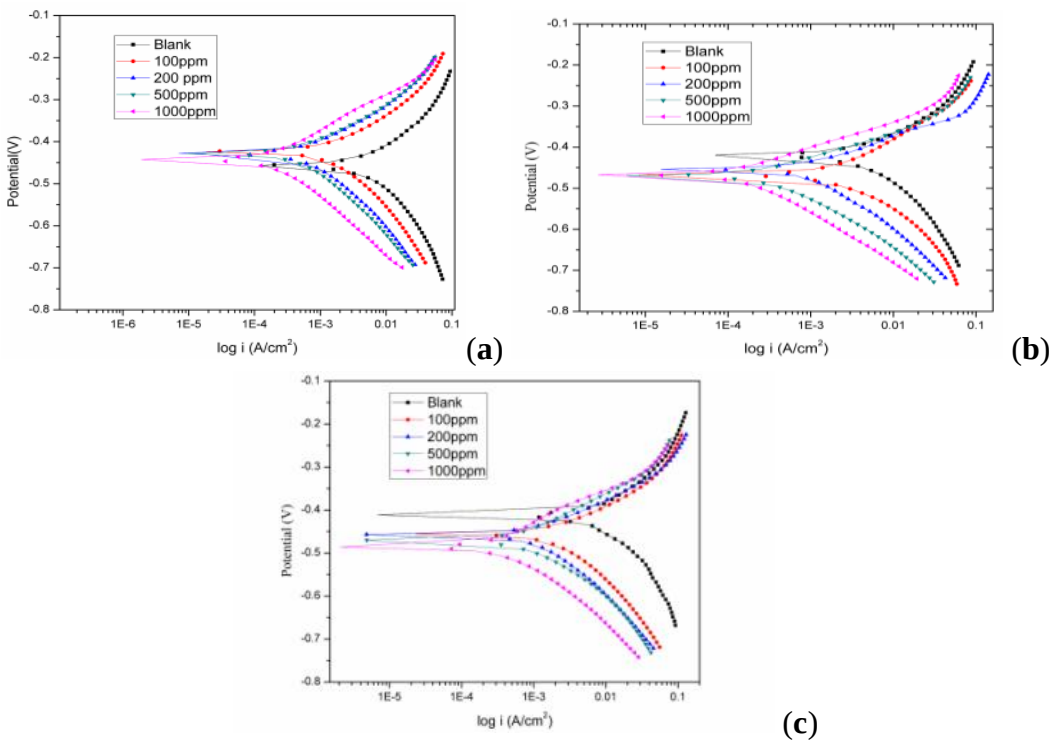

Figure 3. Tafel curve for mild steel in 1M HCl solution at different temperatures **a)** 303 K; **b)** 313 K; **c)** 323 K in the absence and presence of varied HC leaf concentrations.

Table 2. Mild steel polarization data in 1 M HCl at various temperatures along with different concentrations of HC leaves extract.

Temperature of the medium (K)	Concentration of the extract ppm	E corr mV/SCE	I_{corr} (m A/cm^2)	βa (mV/dec)	βc (mV/dec)	ν_{Corr} (mm/yr)	η (%)	Standard Deviation
303	Blank	-457.51	3.251	96.21	110.3	37.81	--	2.3%
	100	-424.3	2.424	130.6	208.3	28.20	25.41	1.1%
	200	-429.2	1.316	126.4	198.9	15.30	59.52	2.1%

Temperature of the medium (K)	Concentration of the extract ppm	E corr mV/SCE	I_{corr} (m A/cm^2)	βa (mV/dec)	βc (mV/dec)	ν_{Corr} (mm/yr)	η (%)	Standard Deviation
	500	-428.7	1.010	115.5	192.1	11.74	68.93	3.8%
	1000	-442.8	0.3185	98.53	153.2	3.705	90.20	2.1%
313	Blank	-418.7	5.370	135.4	209.0	62.46	--	1.9%
	100	-466.4	3.711	152.2	177.6	43.17	30.88	1.7%
	200	-454.0	2.037	87.75	199.6	23.69	62.06	0.66%
	500	-468.8	1.184	102.1	185.2	13.77	77.94	2.6%
	1000	-468.0	0.388	89.29	149.7	4.513	92.77	2.2%
323	Blank	-412.4	7.980	136.7	174.7	92.83	- -	2.1%
	100	-455.2	4.182	124.1	232.9	48.64	47.59	3.4%
	200	-457.5	2.511	109.9	212.3	29.21	68.52	3.1%
	500	-470.8	1.589	117.4	163.7	18.48	80.08	0.98%
	1000	-486.7	0.499	94.73	130.8	5.815	93.73	2.4%

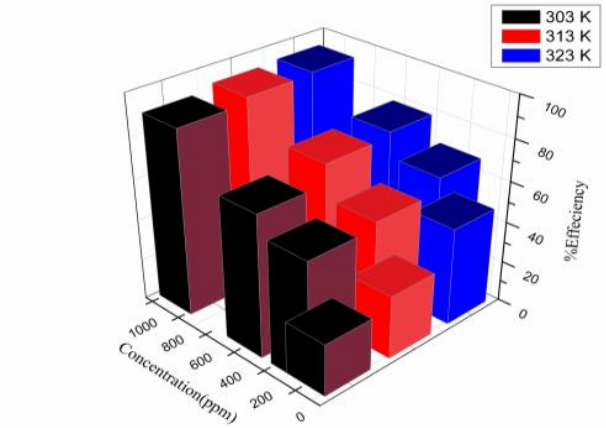

Figure 4. 3D illustration for the variation of the inhibition efficiency at different concentrations of HC leaf extract in 1 M HCl over the temperature range 303-333 K.

Furthermore, by adding the extract to the corrosive medium, the βa and βc values change, indicating that extract controls mild steel corrosion by controlling the dissolution of metals as well as the evolution of hydrogen via adsorption of inhibitor on the active sites of the anode and cathode. So HC extract can be considered a mixed inhibitor form [30,31]. But the study reveals that the change in values of βc is somewhat more prominent than values βa suggesting that studied compounds act as mixed-type inhibitors [32,33].

3.2.3. EIS evaluations.

The corrosion behavior of mild steel in 1 M HCl solution in the presence of HC leaves extract was investigated by EIS at 303K. The fitted Nyquist plots for mild steel in the absence and presence of HC leaves extract in 1 M HCl at 303K as shown in Figure 5(a). Zsimpwin 3.20 Software was employed to analyze all the data in terms of the electrical equivalent circuit. An equivalent circuit to fit the experimental EIS data is shown in Figure 5(b). In the used equivalent circuit, Figure 5(c), R_s is the uncompensated solution resistance R_{ct} refers to the charge transfer resistance, and CPE is the constant phase element.

CPE is often used in the place of a double layer capacitor to obtain a more accurate fit as the C_{dl} do not behave as an ideal capacitor [34]. The impedance of CPE is described by the following formula [35]

$$Z_{CPE} = \frac{1}{Q(j\omega)^n} \qquad (4)$$

where Q is the magnitude also called the CPE constant, **ω** is the angular frequency j^2 = -1 is the imaginary number, and n is the exponential term of a CPE that refers to phase angle, which is applied as an indicator of surface heterogeneity

Accordingly, CPE was used to represent the double layer capacitance (C_{dl}). The value of C_{dl} can be determined from CPE based on the equation [36]

$$C_{dl} = \sqrt[n]{Q \, X \, R_{ct}^{1-n}} \qquad (5)$$

The extract efficiency was obtained using the equation [37]

$$\eta\,(\%) = \frac{R_{ct\,(1)} - R_{ct\,(0)}}{R_{ct(1)}} \times 100 \qquad (6)$$

where $R_{ct(1)}$ and $R_{ct(0)}$ are the charge resistance at individual and zero concentration of inhibitor. The main parameters deduced from an equivalent circuit, such as solution resistance (R_s), charge transfer resistance (R_{ct}), fit goodness (Y^2), double layer capacitance (C_{dl}), phase angle (n), and inhibition efficiency (η (%)) are listed in Table 3.

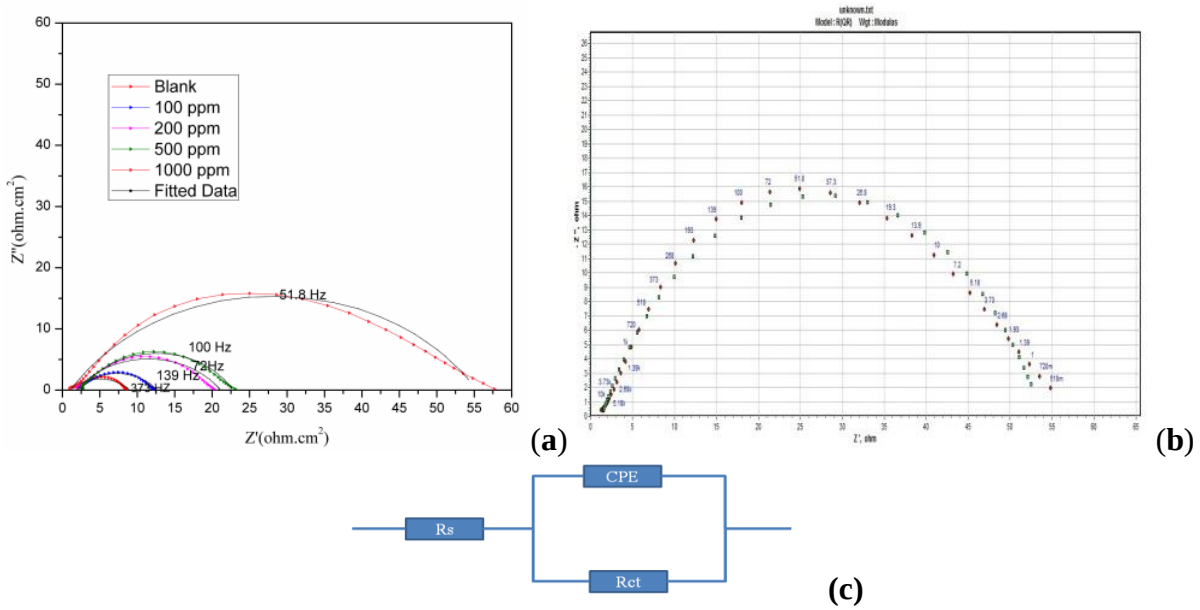

Figure 5. (a) The fitted Nyquist plots for the mild steel corrosion in 1 M HCl with and without various concentrations of HC leave extract at 303 K.**(b)** Equivalent circuit to fit the experimental EIS data. **(c)** The circuit that fits the analyzed EIS data obtained for leaves extracts of HC in 1M HCl solutions.

Table 3. The fitted electrochemical impedance spectroscopy data for the corrosion of mild steel in 1 M HCl solution containing different HC extract concentrations at 303K.

HC Concentration (ppm)	R_s (Ω/cm^2)	R_{ct} (Ω/cm^2)	Q x10-4 ($\Omega^{-1}s^n cm^{-2}$)	n	Y^2	C_{dl} (F) ($\mu F\ cm^{-2}$)	η (%)	Standard Deviation
Blank	1.094	7.888	28.62	0.5492	0.00348	127.43	---	2.8%
100	2.059	10.55	15.38	0.6025	0.00108	101.42	25.23	2.1%
200	1.914	19.18	11.38	0.6212	0.00274	109.54	58.87	3.6%
500	2.429	20.35	6.421	0.6798	0.00197	83.23	61.23	1.3%
1000	1.099	54.22	4.995	0.6559	0.00769	74.64	85.45	2.3%

The Y^2 values were used to evaluate the fitting quality to the electrical equivalent circuit. In all cases, the values of Y^2 were very small, indicating a very high fit between received impedance spectra and the proposed equivalent circuit [38]. This result is attributed to the adsorption of the extract onto the metal /solution interface with increasing concentration [39]. For example, n = 0 represents the resistance, n = 1 represent the capacitance, n = −1 represents the inductance and n = 0.5 represents the Warburg impedance. In our present study, values of n in the absence and presence of inhibitor molecule range from 0.5492 to 0.6798. The deviation from unity (ideal capacitive behavior) is attributed to the presence of surface inhomogeneity and surface roughness[40]. The slight increase in n value in inhibited solution compared to the blank medium can be explained by the adsorption of inhibitor on the steel surface, indicating

that the surface heterogeneity changes insignificantly [41]. In this case, the n value ranging between 0.6025 and 0.6798 indicates that the charge-transfer process controls the dissolution mechanism of mild steel in 1 M HCl solution in the presence of extract. The decreased value of Q in the presence of HC extract is probably due to a decrease in the local dielectric constant and/or an increase in the thickness of the electrical double layer, which decreases the extent of mild steel dissolution. Furthermore, the low values of Q suggest that extract molecules were possibly replacing water molecules at the metal–solution interface. The Nyquist plot contains semicircles with their center located on the x-axis, and their diameter increases with an increase in the concentration of HC leaves extract, indicating a process of charge transfer that controls the corrosion of metal, which insist that extract is adsorbed on the mild steel surface and a stable protecting film is formed on the mild steel surface [42]. Increasing concentrations of extract increase R_{ct} and η (%). Increasing the value of R_{ct} with inhibitor, concentration retards the corrosion rate and suggests effective inhibition performance in the presence of extract [43]. Additionally, a decrease in C_{dl} in the presence of the explored extract is typically explained by a drop in the local dielectric constant and an increase in the thickness of the electrical double layer caused by the displacement of extracted molecules with water molecules during adsorption [44]. The Bode plots (Bode phase plots and Bode modulus plots) obtained for mild steel with and without HC leaves extract containing 1 M hydrochloric acid at 303K are presented in Figure 6 and Figure 7, respectively.

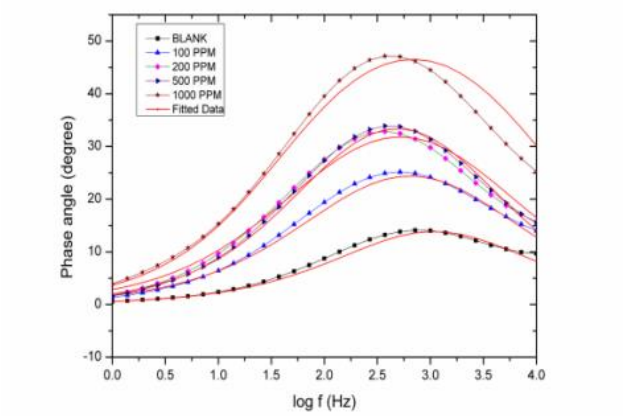

Figure 6. The fitted bode Phase angle plots of mild steel corrosion in 1 M HCl with and without different concentrations HC leave extract 303 K.

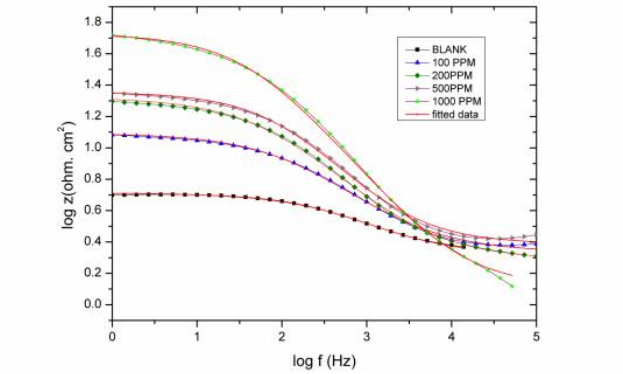

Figure 7. The fitted bode modulus plot for the corrosion of mild steel in 1 M HCl in the absence and presence of different concentrations of HC leaves extract at 303 K.

Phase angle plots for inhibited and uninhibited mild steel are characterized by a single peak, i.e., one constant time at the intermediate frequencies, whose broadening in the presence of inhibitors molecules indicates the formation of a protective film on the steel specimens [45

46]. Bode diagrams also show that the impedance modulus and the phase angle increase with inhibitor concentration because of the upsurge of inhibitor adsorption on the mild steel surface [47, 48]. According to the literature, an ideal capacitor would show a slope value of −1 and a phase angle value of −90°. In the present study, a deviation from the ideal case is attributable to the surface inhomogeneity and roughness arising from corrosion [49]. The standard deviation of efficiency for mass loss, EIS, and PDP at various temperatures is shown in Figure 8 in the form of a bar chart.

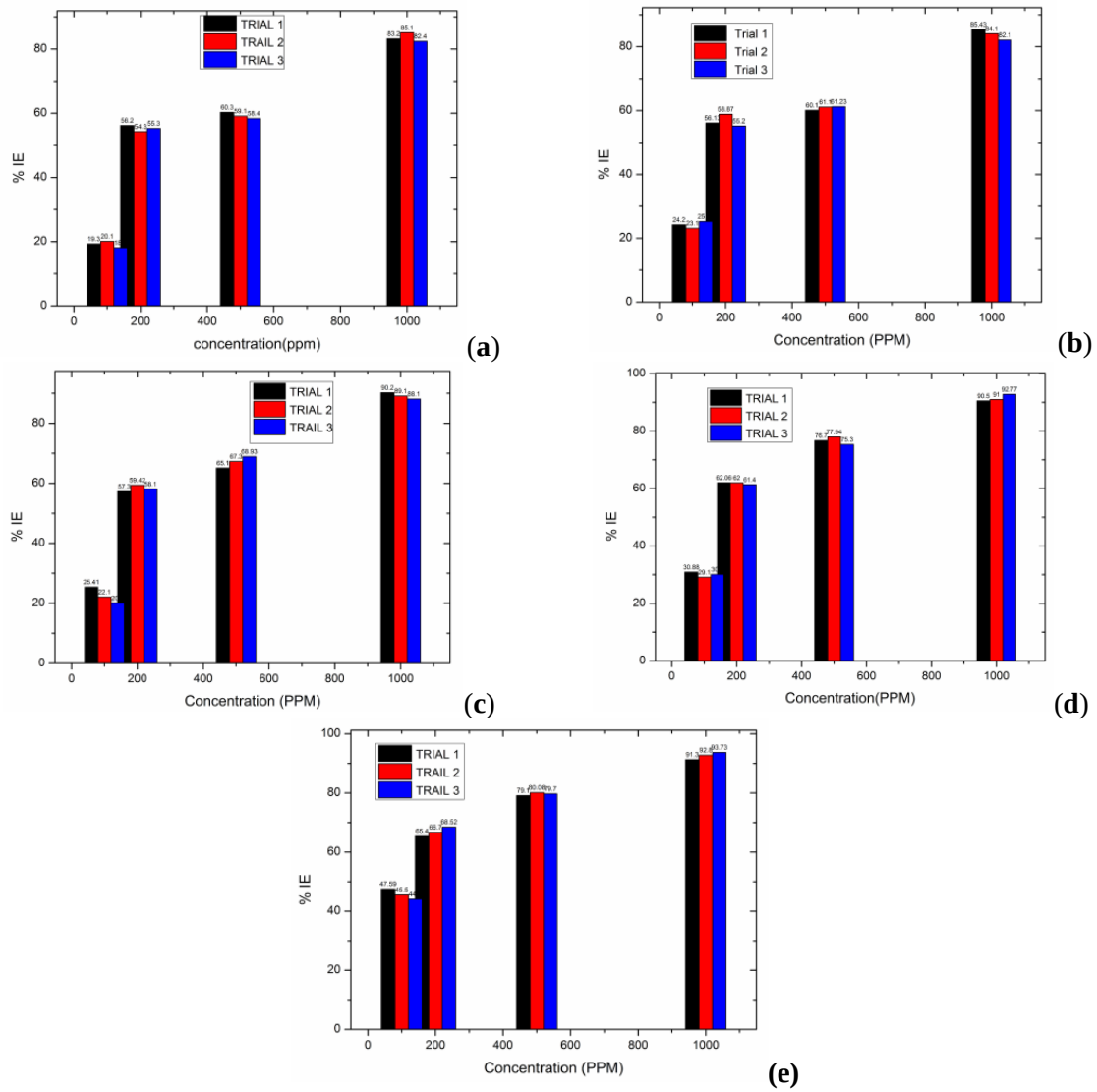

Figure 8. Standard deviation in terms of a bar chart for **(a)** mass loss; **(b)** EIS; **(c)** PDP at 303 K; **(d)** PDP at 313 K; **(e)** PDP at 323 K.

3.3. Adsorption model analysis.

The adsorption isotherm will provide basic details on how inhibitors interact with mild steel surfaces. The ideal isotherm was recognized using the surface coverage values at different concentrations of HC leaves extract in acid media at varying temperatures (303–323 K) to determine the adsorption process. Various adsorption isotherms were fitted to the data between surface coverage θ and concentration C (mg/L) of inhibitors, including the Langmuir, Temkin, Frumkin, and Freundlich isotherms. According to this isotherm, surface coverage θ and concentration of inhibitor are linked together by the following equations are expressed as follows [13, 50].

$$\frac{C_{inh}}{\theta} = \frac{1}{K_{ads}} + C_{inh} \quad \text{(Langmuir isotherm plot of } \frac{C_{inh}}{\theta} \text{ vs. } C_{inh}\text{)} \quad (7)$$

$$\theta = \frac{2.303}{\alpha}(\log K_{ads} + \log C) \quad \text{(Temkin isotherm plot of } \theta \text{ vs. } \log C\text{)} \quad (8)$$

$$\log \frac{\theta}{(1-\theta)} = y \log C + \log K \quad \text{(El-Awady isotherm plot of } \frac{\theta}{(1-\theta)} \text{vs. } \log C\text{)} \quad (9)$$

$$\log \theta = n \log C + \log K_{ads} \quad \text{(Freundlich isotherm plot } \log \theta \text{ vs. } \log C\text{)} \quad (10)$$

Linear relationships for all tested isotherms are shown in Figures 9-12. R^2 values for the various adsorption isotherms are listed in Table 4. Langmuir isotherm has a maximum regression coefficient (R^2) that is very close to 1, indicating that the Langmuir model is suitable for describing the adsorption process. Langmuir adsorption confirms the formation of a monolayer on the mild steel surface, and there is no interaction between the adsorbed extract on the mild steel surface [51]. Therefore Langmuir plot is appropriate for evaluating the adsorption equilibrium constant K_{ads}. The Langmuir isotherm provides a straight line that does not pass through the origin, signifying the non-ideal behavior of HC extract in the absorption process [52]. The higher value of K_{ads} suggests that the process of adsorption is preferred by the forward direction. Hence it infers a strong interaction between the metal surfaces and extracts [53].

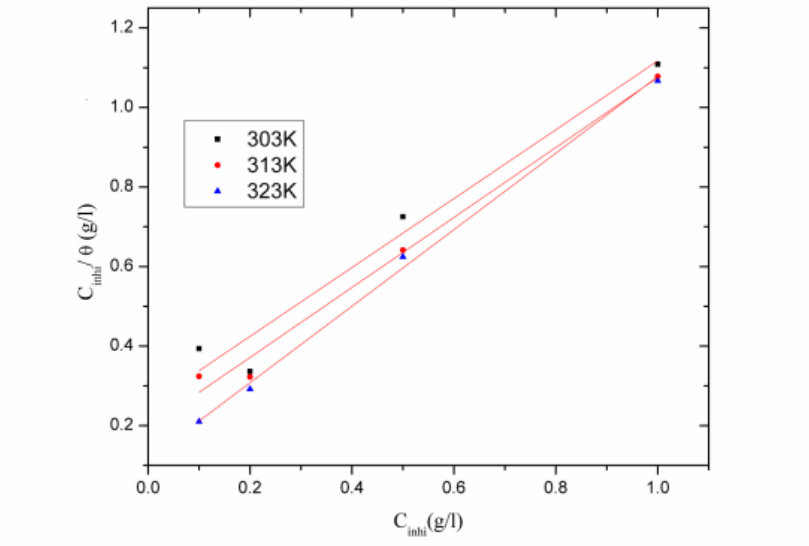

Figure 9. Langmuir isotherm plot $\frac{C_{inh}}{\theta}$ vs. C_{inh}.

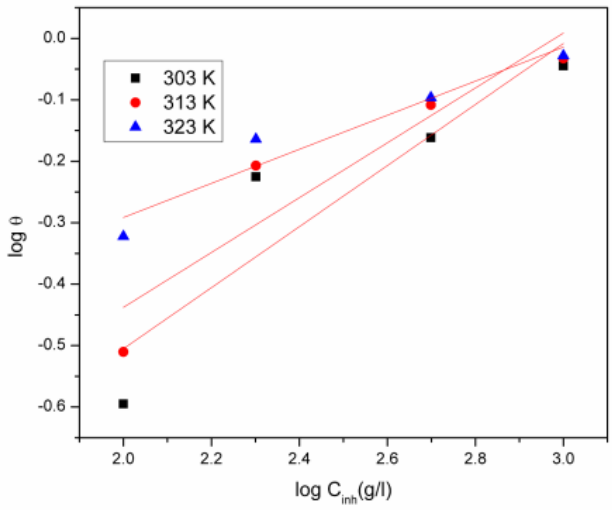

Figure 10. Freundlich isotherm plot($\log \theta$ vs. Log C)

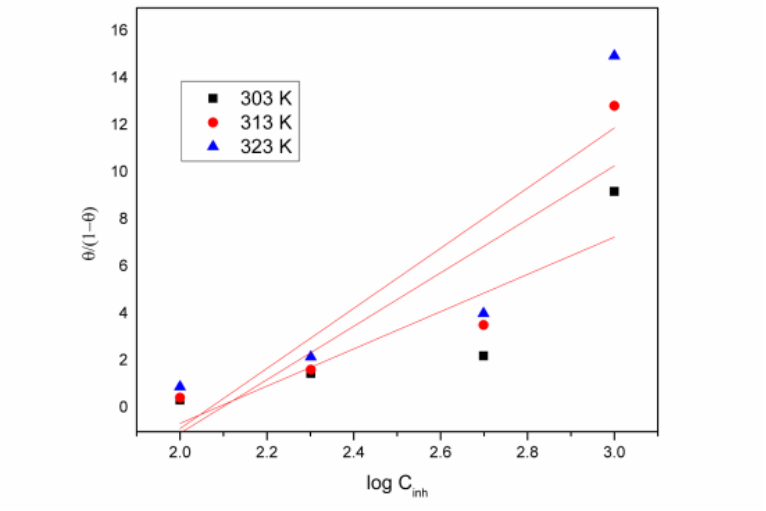

Figure 11. El-Awady isotherm plot $\frac{\theta}{(1-\theta)}$ vs. log C.

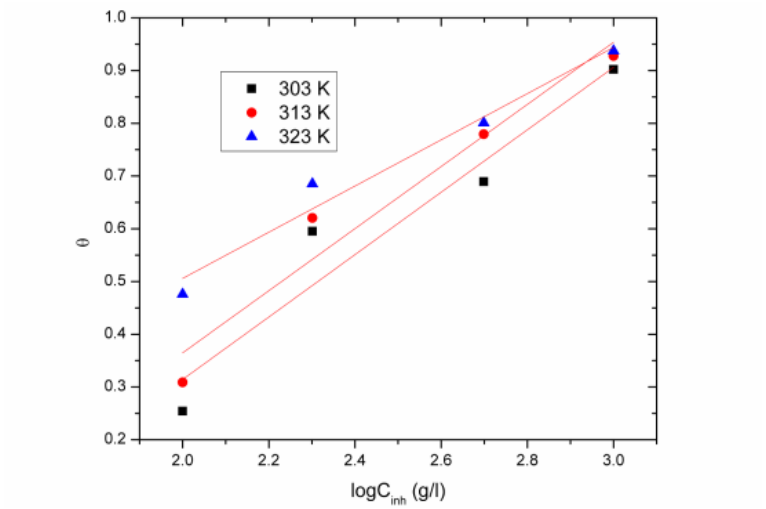

Figure 12. Temkin isotherm plot (θ vs. log C).

Table 4. R^2 values of different adsorption isotherms for HC leaves extract.

Temperature of the medium (°C)	Langmuir	Temkin	El-Awady	Freundlich
	R^2	R^2	R^2	R^2
30	0.949	0.892	0.6289	0.766
40	0.983	0.928	0.6774	0.812
50	0.996	0.956	0.6432	0.903

Table 5. Langmuir isotherm parameters for mild steel in 1M HCl containing various concentrations of the HC leaves extract at different temperatures.

Temperature of the medium (°C)	ΔG^0ads(kJ/mol)	K_{ads} (L /g)
30	-30.99	3980.1
40	-32.67	5114.0
50	-35.13	8673.7

The obtained values of K_{ads} from the Langmuir, adsorption is related to the free energy of adsorption ΔG°_{ads} according to the following equation [54]

$$\Delta G^{\circ}_{ads} = -RT \ln(55.5 K_{ads}) \qquad (11)$$

The values of K_{ads} and ΔG°_{ads} are given in Table 5. The negative value ΔG°_{ads} indicates the stability of the adsorbed layer on the steel surface and the spontaneity of the adsorption process. In general, electrostatic interactions between an inhibitor and a charged metal surface (physisorption) are typically thought to occur at a magnitude of ΔG°_{ads} around -20 kJ / mol or

less negative. Whereas Chemisorption results around -40 kJ / mol or more negative are indicative of charge sharing from organic species to the metal surface, leading to a coordinate type of metal bond [55, 56]. The obtained free energy of adsorption (ΔG°_{ads}) for HC leaves extract ranges from -30.1 to -35.1 kJ/mol. So extract behave as a mixed type (physiochemisorption) [57]. But ΔG°_{ads} value is moderately nearer to -40 kJ/mol. Therefore, an extract is predominantly adsorbed on the mild steel surface by a chemisorption mode [58].

3.4. Thermodynamic activation parameters.

Interaction between the mild steel electrode and the acidic media without and with the extract can be altered by temperature. The mechanism of inhibition can be understood from the data obtained from the thermodynamic aspects. The dependency of the corrosion rate on temperature can be exhibited by the Arrhenius equation and transition-state equation as [59]

$$\ln C_R = \ln A - \left[\frac{E_a^{\#}}{RT}\right] \qquad (12)$$

$$\ln \frac{C_R}{T} = \left[\ln \frac{R}{Nh} + \frac{\Delta S_a}{R}\right] - \frac{\Delta H_a}{R} \qquad (13)$$

where $E_a^{\#}$apparent activation energy, T absolute temperature, A Arrhenius pre-exponential factor, R is the gas constant and C_R is the corrosion rate. N is Avogadro's number, and h is Planck's constant. The $E_a^{\#}$ values can be determined from the slop of Arrhenius plots ln C_R vs. 1/T as shown in Figure 13. The plot of ln $\frac{C_R}{T}$ vs $\frac{1}{T}$ Figure 14 gives a straight line with a slope of - $\frac{\Delta H_a}{R}$ and the intercept $\ln \frac{R}{Nh} + \frac{\Delta S_a}{R}$, from which ΔH_a and ΔS_avalues were measured. The calculated $E_a^{\#}$, ΔH_a , ΔS_a are shown in Table 6. It is frequently assumed that an increase in inhibition efficiency with temperature rise, coupled with the decrease in corrosion activation energy in the presence of inhibitors compared to their absence, is indicative of the formation of chemically adsorption films. Specifically, the mechanism ascribed to the lower inhibition efficiency with temperature increase, and a corresponding increase in corrosion activation energy in the presence of inhibitors compared to their absence, is described as physical adsorption [57].

Table 6. Activation parameters for mild steel corrosion in 1 M HCl in the absence and presence of different concentrations of HC leave extract.

SJ Concentration ppm	$E_a^{\#}$ (kJ/mol)	ΔH_a(kJ/mol)	ΔS_a(Jmol^{-1}K^{-1})
Blank	36.57	33.97	-102.6
100	22.29	19.69	-151.8
200	26.38	23.78	-143.5
500	18.37	15.77	-172.6
1000	18.30	15.70	-182.4

From the obtained results in Table 6, it is clear that $E_a^{\#}$ values in the presence of the different concentrations of the extract are lower than in their absence. Such behavior, coupled with the trend of increased inhibition efficiency, is evidence of chemisorptions [60]. Enthalpy of activation $\Delta H_a$is positive for all the extract concentrations, reflecting the endothermic nature of the mild steel dissolution process, i.e., dissolution of mild steel is slow in the presence of extract, and the endothermic process is attributed to chemisorptions [61]. The negative values

of ΔS_a indicate that the extract molecules form a stable film and are adsorbed orderly onto the mild steel surface [62]. It is well noticed that the values of $E_a^{\#}$ are greater than the analogous values of H_a suggesting that the corrosion process involved a gaseous reaction, simply the hydrogen evolution reaction, associated with a decrease in the total reaction volume [63].

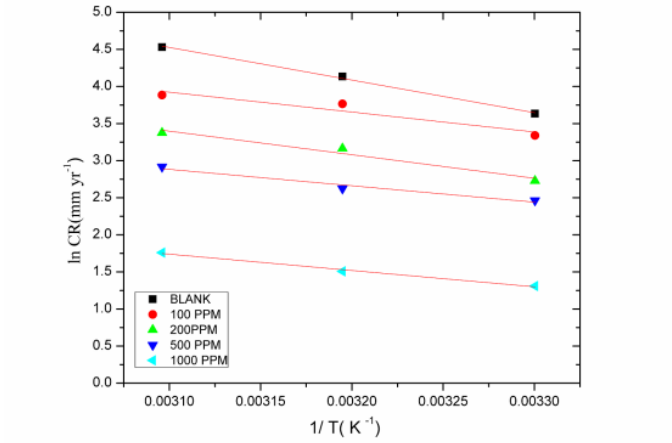

Figure 13. Adsorption isotherm plot for ln CR vs. 1/T.

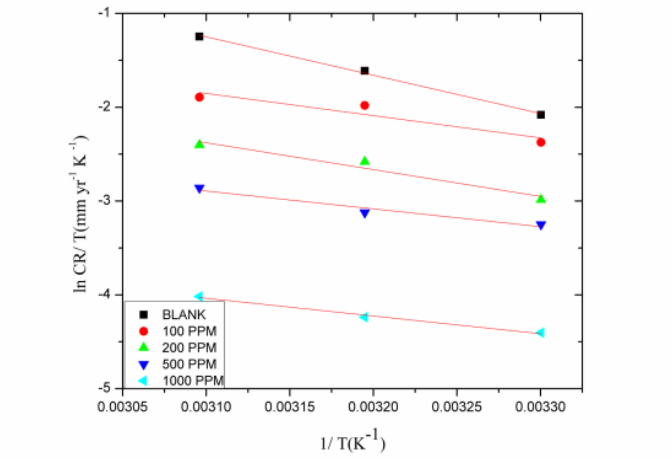

Figure 14. Adsorption isotherm plot for ln (C R /T) vs. 1/T.

In addition, the average difference value of the $E_a^{\#}$-ΔH_a is 2.6kJ/mol which is approximately around the average value of RT (2.63 kJ/mol). Hence corrosion process is indicated as a unimolecular reaction with the evolution of hydrogen gas, as is defined by the equation [12]

$$E_a^{\#} - \Delta H_a = RT \qquad (14)$$

3.5. Surface morphology of test specimen.

3.5.1. Scanning electron microscopy.

The scanning electron microscope images were recorded to establish the interaction of extract molecules with the metal surface. Figures 15(a) and 15(b) depict the morphologies of mild steel specimens after immersion for 24 hours in 1M HCl solutions without and with 1000ppm of HC leaves extract. It can be observed that the surface of mild steel in the absence of the extract (Figure 15(a)) is highly damaged, there is the formation of different forms of corrosion products (iron oxides) on the surface in the absence of the extract and a scale-like black corrosion product covers the entire surface. However, in the presence of the extract, the damage to the steel surfaces is significantly reduced (Figure 15(b)) reveals that the plant extract

forms a protective film on metal surfaces which prevents the dissolution of mild steel in acid media by forming a surface adsorbed layer.

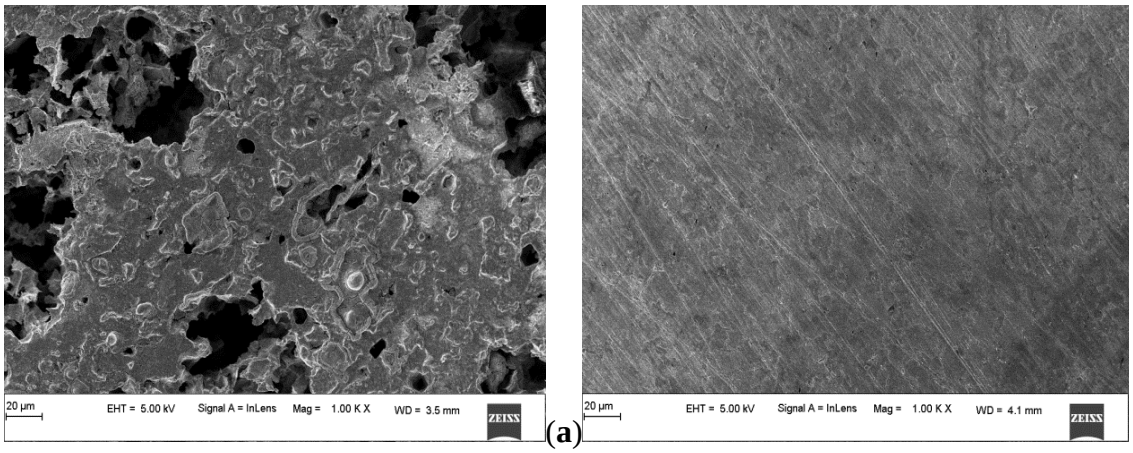

(**a**) (**b**)

Figure 15. SEM image of Mild steel surface **(a)** immersed in 1M HCl for 24 hours **(b)** immersed in 1M HCl in the presence of 1000 ppm HC leaf extract for 24 hours.

3.6. Energy-dispersive X-ray spectroscopy.

EDX images of the uninhibited and inhibited mild steel samples are shown in Figures 16(a) and 16(b), respectively. In the presence of the inhibitor, the intensity oxygen peak is suppressed considerably. The suppression of the oxygen peak and enhancement in the intensity of iron peak is attributed to the inhibitor film on the mild steel specimen, indicating the adsorption of extract molecule on mild steel surface, forming a protective layer between mild steel and acid solution and preventing dissolution of metal ions in the aggressive medium [64-66]. By adding this HC extract, the O/Fe ratio has also decreased. This confirms the inhibitory behavior of extract against the corrosion of mild steel in 1 M HCl.

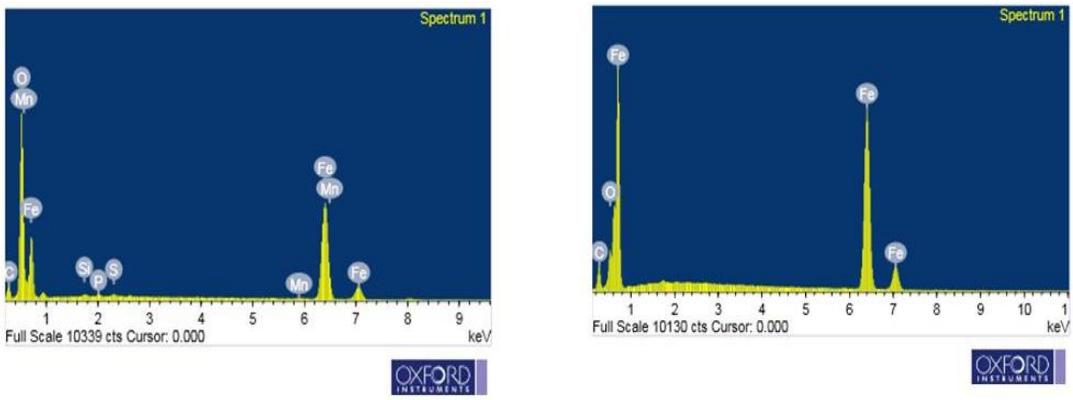

(**a**) (**b**)

Figure 16. EDX image **(a)** mild steel exposed in 1 MHCl and **(b)** mild steel exposed in 1 M HCl in the presence of 1000 ppm of HC leaf extract.

3.7. Extract characterizations.

3.7.1. FT-IR spectroscopy.

FT-IR analysis was performed to identify the functional groups present in the extract and the corrosion product and to confirm the inhibition due to the interaction between the extract and metal. IR spectrum of the extract and extract adsorbed on the surface of mild steel is illustrated in Figure 17. The peak located at 3296.34 cm^{-1} corresponds to O-H stretching in alcohol. The peak at 2517.10 cm^{-1} was assigned to O-H stretching in a carboxylic acid. The peak that appeared at 1581.6cm^{-1} is attributed to the N-H bend. The further peak at 1429.2 cm^{-}

[1] is due to the aromatics ring's C-H stretching, and peaks at 1244.08 assigned have C–N stretch in aliphatic amines. C-O stretching was noted at 1049 cm^{-1}.

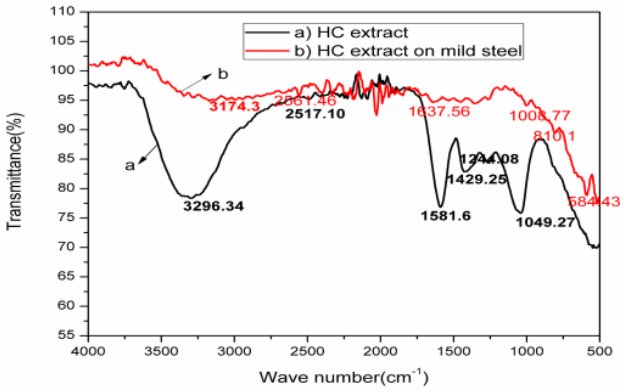

Figure 17. FTIR spectra of HC leaves extract and extract absorbed on the mild steel surface.

The prevalence of functional groups in extracts of HC is an indication of corrosion inhibition characteristics. In the case of HC extract adsorbed on mild steel, it does not show characteristic peaks. Many functional groups in the adsorbed film were missing, indicating protective film formation on the mild steel surface. This is due to the formation of bonds with Fe in mild steel in 1M HCl, making HC extract enviable for corrosion inhibition performance.

3.8. UV analysis.

UV-visible analysis confirms the complexing property of HC extract with the ions dissolved in the corrosive solution [67]. UV–visible spectra before and after immersion of mild steel samples in 1 M HCl solution containing 1 g/L HC extract with an immersion period of 10 hours were reported in Figure 18. In the UV-visible spectra, the appearance of one or more peaks in the region from 200 to 400 nm is a clear indication of the presence of unsaturated groups and heteroatom [68]. From the UV spectra, the absorbance of the corrosive medium before the corrosion test is higher than the absorbance of the corrosive medium after the corrosion test. It shows that some molecules from the solution have been adsorbed on the metal surface when a mild steel sample was immersed into the acidic solution of HC extract. The change in the absorbance value recommended the formation of a complex between the iron and phytochemicals of HC extract [69]. Also, a significant change in the shape of the spectra before and after immersion of mild steel indicates the possibility of forming an inhibitor layer over the mild steel surface [70]. This prompts us to conclude that there is a possibility of forming a complex between phytochemicals of HC extract and the iron ion, which contributes to the inhibitive action.

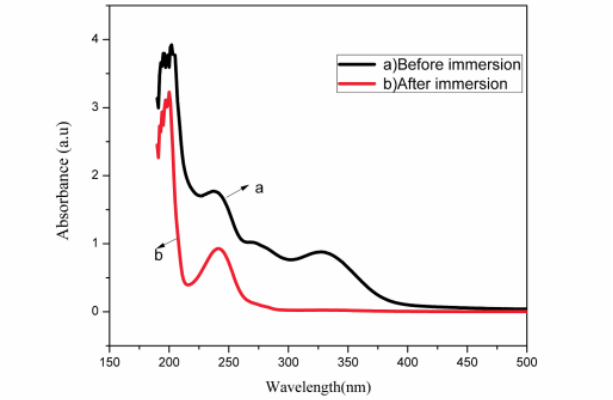

Figure 18. UV-Visible spectrum for HC leaf extract in the absence and presence of mild steel.

3.9. Mechanism of corrosion inhibition.

The interface between metal and corrosion solution in free acid is an active dissolution state. Corrosion protection mainly depends on the concentration of the corrosive medium, stability, molecular size, adsorption centers, electronic structure of the inhibitor, and so on. HC leaves extract is rich in flavonoids, phenolic acid, alkaloids, and carbohydrates [19]. These phytochemicals contain heteroatoms like S, O, N, H, etc. These heteroatoms tend to reduce or inhibit the metals dissolution process. The extract molecules can be adsorbed on the mild steel chemically, physically, or through both mechanisms. The adsorption process of the inhibitor is a displacement reaction, where the molecules of the inhibitor replace the water molecules on the metal surface, which can be expressed according to the following equation [71]

$$Inh\ (sol) + n\ H_2O\ (ads) \longleftrightarrow Inh\ (ads) + H_2O\ (sol)$$

In the present work, the HC leaf extract contains many phytocompounds; hence it is difficult to describe a particular component responsible for corrosion inhibition activity. Figure 19 shows the schematic diagram of corrosion protection of mild steel dipped in 1 M HCl medium with HC leaf extract.

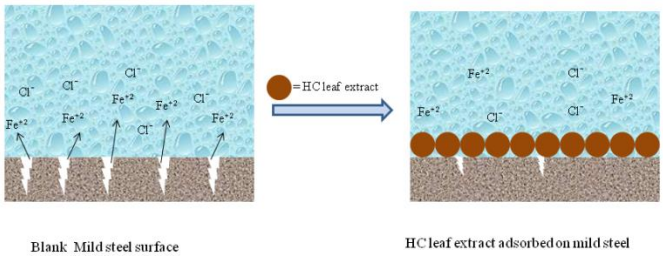

Figure 19. The schematic diagram for the adsorption of HC leaf extract on a mild steel surface.

The adsorption model analysis and thermodynamic activation parameters show that inhibition activity of phytocompounds from HC leaf extract is typically a mixed type with predominantly chemical adsorption. Hence photochemical constituents are effectually adsorbed on mild steel surfaces forming a protective layer and acting as eco-friendly effective corrosion inhibitors

3.10. Comparative efficiency study.

The inhibition efficiency of the HC leave extract is compared with other green corrosion inhibitors reported in the literature. Anti-corrosion efficiency of Allium sativum [72] extract has been examined for mild steel in 1 M HCl; its protection efficiency was found to be 76.47%. *Xylopia ferruginea* [73] also showed 93% inhibition efficiency on mild steel in 1M HCl. Henna extracts [74] exhibited 92.06% corrosion inhibition efficiency for mild steel in 1 M HCl. The inhibitive action of Aspilia Africana [75] leaves extract on the corrosion of mild steel in 1M HCl solution at room temperature and 60ºC. The mass loss technique studied it and showed good inhibition efficiency values of 88.1% at room temperature and 91% at 60°C. The inhibition potential of aqueous extract of *Pisum sativum* (green pea) peels [76] for corrosion of mild steel showed inhibition efficiency of 91% for mass loss; 87% for polarization method, and 90% for EIS in 1 M HCl at 400 mg/L extract concentration. This study obtained the highest inhibition efficiency values of 90.2 % at 313 K and 93.7% at 323 K with 1000ppm of HC leaves extract on mild steel. Hence aqueous extract of HC leaf is considered a novel, high-performance, renewable, eco-friendly green corrosion inhibitor.

Another important point is that unlike aqueous phase extraction of HC leave extract, non-aqueous solvents are necessary for extracting many of the green inhibitors, which increases the cost and leaves negative environmental impacts. But the present study has focused on the low-cost corrosion inhibition performance of leaf extracts from an environmental viewpoint to avoid negative impacts from non-aqueous solvents. Besides, phytocompounds from HC leaf extracts can be naturally biodegradable along with their simple and safe extraction process.

4. Conclusions

A new green aqueous extract of Hemigraphis Colorata leaf showed a significant corrosion inhibition activity in 1 M HCl in the current study. Electrochemical experiments revealed the concentration-dependent protection inhibition efficacy of HC leaves extract. The inhibition efficiency of the extract by PDP, EIS, and mass loss methods was found to be 90.2 %, 85.45%, and 85.1%, respectively, at 1000 ppm for 303 K. The inhibition efficiency of HC leaf extract improved with higher concentration and higher temperatures. Temperature effect shows that HC leaves extract exhibited a maximum efficiency of 93.73 % at 323 K. From an environmental viewpoint, aqueous extract HC leaf is considered a novel, non-toxic, renewable, economic, eco-friendly green corrosion inhibitor for mild steel in 1 M HCl as it avoids negative impact from non-aqueous solvents. Due to its biodegradability and eco-friendliness, HC leaves extract gained significant attention regarding corrosion prevention. Potentiodynamic polarization study revealed that the investigated extracts are mixed-type inhibitors with predominantly cathodic inhibitive effects. The HC leaf exhibited monolayer surface coverage and was confirmed by the Langmuir isotherm. The negative value ΔG°_{ads} suggests the stability of the adsorbed layer on the mild steel surface, and HC leaves extract adsorbed spontaneously on the mild steel surface. The calculated adsorption energy of extract is found to be in the range of -30.1 to -35.1 kJ/mol, which indicates extract is adsorbed on the metal surface by both physisorption and chemisorption mechanisms. FTIR and UV-visible spectroscopy analyses indicated that the extract molecules were adsorbed on the mild steel surface to form a protective layer. SEM and EDX analysis provided evidence for forming a protective film of HC leaf extract on a mild steel surface, which shields the metal surface from direct contact with the acidic environment.

Funding

This research received no external funding.

Acknowledgments

Declared none.

Conflicts of Interest

The authors declare no conflict of interest.

References

1. Sanni, O.; Fayomi, O.; S. I.; & Popoola, A. P. I. Eco-friendly Inhibitors for Corrosion Protection of Stainless steel: An Overview. *J Phys: Conf Ser* **2019**, *1378*, 042047, https://doi.org/10.1088/1742-6596/1378/4/042047.

2. Fakhry, H.; El Faydy, M.; Benhiba, F.; Laabaissi, T.; Bouassiria, M.; Allali, M.;& Zarrouk, A. A newly synthesized quinoline derivative as corrosion inhibitor for mild steel in molar acid medium: Characterization (SEM/EDS), experimental and theoretical approach. *Colloids Surf A Physicochem Eng Aspects* **2021**, *610*, 125746, https://doi.org/10.1016/j.colsurfa.2020.125746.
3. Zinad, D. S.; Jawad, Q. A.; Hussain, M. A. M.; Mahal, A.; Mohamed, L.; Al-Amiery, A. A. Adsorption, temperature and corrosion inhibition studies of a coumarin derivatives corrosion inhibitor for mild steel in acidic medium: gravimetric and theoretical investigations. *Int J Corros Scale Inhib* **2020**, *9*, 134-151, https://doi.org/10.17675/2305-6894-2020-9-1-8.
4. Singh, A. K.; Chugh, B.; Saha, S. K.; Banerjee, P.; Ebenso, E. E.; Thakur, S.; Pani, B. Evaluation of anti-corrosion performance of an expired semi synthetic antibiotic cefdinir for mild steel in 1 M HCl medium: An experimental and theoretical study. *Results in Phys* **2019**, *14*, 102383, https://doi.org/10.1016/j.rinp.2019.102383.
5. Marzorati, S.; Verotta, L.; Trasatti, S. P. Green corrosion inhibitors from natural sources and biomass wastes. *Molecules* **2019**, *24*, 48, https://doi.org/10.3390/molecules24010048.
6. Belghiti, M. E.; Echihi, S.; Dafali, A.; Karzazi, Y.; Bakasse, M.; Elalaoui-Elabdallaoui, H.; Tabyaoui, M. Computational simulation and statistical analysis on the relationship between corrosion inhibition efficiency and molecular structure of some hydrazine derivatives in phosphoric acid on mild steel surface. *Appl Surf Sci* **2019**, *491*, 707-722, https://doi.org/10.1016/j.apsusc.2019.04.125.
7. Bharatiya, U.; Gal, P.; Agrawal, A.; Shah, M.; Sircar, A. Effect of corrosion on crude oil and natural gas pipeline with emphasis on prevention by ecofriendly corrosion inhibitors: A comprehensive review. *J Bio-Tribo-Corros* **2019**, *5*, 1-12, https://doi.org/10.1007/s40735-019-0225-9.
8. Bahlakeh, G.; Ramezanzadeh, B.; Dehghani, A.; Ramezanzadeh, M. Novel cost-effective and high-performance green inhibitor based on aqueous Peganum harmala seed extract for mild steel corrosion in HCl solution: Detailed experimental and electronic/atomic level computational explorations. *J Mol Liq* **2019**, *283*, 174-195, https://doi.org/10.1016/j.molliq.2019.03.086.
9. Miralrio, A.; Espinoza Vázquez, A. Plant Extracts as Green Corrosion Inhibitors for Different Metal Surfaces and Corrosive Media: A Review. *Processes* **2020**, *8*, 942, https://doi.org/10.3390/pr8080942.
10. Hanoon, M.; Zinad, D. S.; Resen, A. M.; Al-Amiery, A. A. Gravimetrical and surface morphology studies of corrosion inhibition effects of a 4-aminoantipyrine derivative on mild steel in a corrosive solution. *Int J Corros Scale Inhib* **2020**, *9*, 953-966, https://doi.org/10.17675/2305-6894-2020-9-3-10.
11. Fouda, A. S.; El-Shereafy, E. E.; Hathoot, A. A.; El-bahrawi, N. M. Corrosion inhibition of aluminum by cerumium rubrum extract in hydrochloric acid environment. *J Bio- Tribo-Corros* **2020,** *6*, 1-16, https://doi.org/10.1007/s40735-020-0330-92.
12. Akinbulumo, O. A.; Odejobi, O. J.; Odekanle, E. L. Thermodynamics and adsorption study of the corrosion inhibition of mild steel by Euphorbia heterophylla L. extract in 1.5 M HCl. *Results Mater* **2020**, *5*, 100074, https://doi.org/10.1016/j.rinma.2020.100074.
13. Aralu, C.C.; Chukwuemeka-Okorie, H.O.; Akpomie, K.G. Inhibition and adsorption potentials of mild steel corrosion using methanol extract of Gongronema latifoliuim. Appl Water Sci **2021**, *11*, 22, https://doi.org/10.1007/s13201-020-01351-85.
14. Raja, P. B.; Fadaeinasab, M.; Qureshi, A. K.; Rahim, A. A.; Osman, H.; Litaudon, M.; Awang, K. Evaluation of green corrosion inhibition by alkaloid extracts of Ochrosia oppositifolia and isoreserpiline against mild steel in 1 M HCl medium. *Ind Eng Chem Res* **2013**, *52*, 10582-10593, https://doi.org/10.1021/ie401387s.
15. Singh, A.; Singh, V. K.; Quraishi, M. A. Inhibition of mild steel corrosion in HCl solution using Pipali (Piper longum) fruit extract. *Arabian J Sci Eng* **2013**, *38*, 85-97, https://doi.org/10.1007/s13369-012-0409-9.
16. Beenakumari, K. S. Inhibitory effects of Murraya koenigii (curry leaf) leaf extractonthecorrosion of mild steel in 1 M HCl. *Green Chem Lett Rev* **2011**, *4*, 117-120, https://doi.org/10.1080/17518253.2010.514866.
17. Anupama, K. K.; Ramya, K.; Joseph, A. Electrochemical and computational aspects of surface interaction and corrosion inhibition of mild steel in hydrochloric acid by Phyllanthus amarus leaf extract (PAE). *J Mol Liq* **2016**, *216*, 46-155, https://doi.org/10.1016/j.molliq.2016.01.019.
18. Okafor, P. C.; Ebenso, E. E.; Ekpe, U. J. Azadirachta indica extracts as corrosion inhibitor for mild steel in acid medium. *Int J Electrochem Sci* **2010**, *5*, 78-993, http://electrochemsci.org/papers/vol5/5070978.pdf.
19. Sushma, M. S. M.; Lahari, S. L. S.; Naidu, M. J. N. M. J.; Kavitha, G. K. G. BIOLOGICAL EFFECTS OF HEMIGRAPHIS ALTERNATE–A REVIEW. *Inte J of Indig Herbs Drugs* **2020**, *5*, 27-30, https://www.saap.org.in/journals/index.php/herbsanddrugs/article/view/87.

20. Safna, M. I.; Visakh, U. V.; Gangadharan, A. Biological activity of hexane extract of Hemigraphis colorata, an indigenous wound healing plant. *Mater Today Proc* **2020**, *25*, 294-297, https://doi.org/10.1016/j.matpr.2020.01.461.
21. Adangampurath, S.; Sudhakaran, S. Anti-inflammatory potential of flavonoids from Hemigraphis colorata. *Int J of Life Sci* **2018**, *6*, 569-574.
22. Santhosh, N. A.; George, M. K. C. L.; Santhosh, N. A. Ecofriendly Synthesis Of Silver Nanoparticles Using Aqueous Leaf Extracts of Hemigraphis Colorata (Blume) Hallier f. And Their Antibacterial Activity. *IJRASET* **2018**, *6*, 2630-2635, http://dx.doi.org/10.22214/ijraset.2018.3588.
23. Joyson, A.; Krishnakumar, K.; Hareeshbabu, E. Hemigraphis colorata: A review. *J Bio Innov* **2017**, *6*, 557-561, https://www.jbino.com/docs/Issue04_07_2017.pdf.
24. Sharma, U. R.; Sharma, N. Green Synthesis, Anti-cancer and Corrosion Inhibition Activity of Cr2O3 Nanoparticles. *Biointerf Res Appl Chem* **2021**, *11*, 8402-8412, https://doi.org/10.33263/BRIAC84028412.
25. Li, D.; Zhang, P.; Guo, X.; Zhao, X.; Xu, Y. (2019). The inhibition of mild steel corrosion in 0.5 MH 2 SO 4 solution by radish leaf extract. *RSC Advances* **2019**, *9*, 40997-41009, https://doi.org/10.1039/C9RA04218K.
26. Karki, N.; Neupane, S.; Gupta, D. K.; Das, A. K.; Singh, S.; Koju, G. M.; Yadav, A. P. Berberine isolated from Mahonia nepalensis as an eco-friendly and thermally stable corrosion inhibitor for mild steel in acid medium. *Arab J Chem* **2021**, *14*, 103423, https://doi.org/10.1016/j.arabjc.2021.103423.
27. Casaletto, M. P.; Figa, V.; Privitera, A.; Bruno, M.; Napolitano, A.; Piacente, S. Inhibition of Cor-Ten steel corrosion by "green" extracts of Brassica campestris. *Corros Sci* **2018**, *136*, 91-105, https://doi.org/10.1016/j.corsci.2018.02.059.
28. Zulfareen, N.; Venugopal, T.; Kannan, K. Experimental and Theoretical Studies on the Corrosion Inhibition of Brass in Hydrochloric Acid by N-(4-((4-Benzhydryl Piperazin-1-yl) Methyl Carbamoyl) Phenyl) Furan-2-Carboxamide. *Int J Corros* **2018**, 1-18, https://doi.org/10.1155/2018/9372804.
29. Bangera, S.; Alva, V. D. Aqueous Extract of Macaranga Peltata Leaves—Green Corrosion Inhibitor for Mild Steel in Hydrochloric Acid Medium. *Surf Eng Appl Electrochem* **2020**, *56*, 259-266, https://doi.org/10.3103/S1068375520020040.
30. Guruprasad, A.M. ; Sachin, H.P.; Swetha, G.A.; Prasanna, B.M. Adsorption and inhibitive properties of seroquel drug for the corrosion of zinc in 0.1 M hydrochloric acid solution. *Int J Ind Chem* **2019**, *10*, 17-30, https://doi.org/10.1007/s40090-018-0168-x.
31. Iroha, N. B.; Madueke, N. A.; Mkpenie, V.; Ogunyemi, B. T.; Nnanna, L. A.; Singh, S.; Ebenso, E. E. Experimental, adsorption, quantum chemical and molecular dynamics simulation studies on the corrosion inhibition performance of Vincamine on J55 steel in acidic medium. *J Mol Struct* **2021**, *1227*, 129533, https://doi.org/10.1016/j.molstruc.2020.129533.
32. Abdallah, M.; Fawzy, A.; Al Bahir, A. The Effect of Expired Acyclovir and Omeprazole Drugs on the Inhibition of Sabic Iron Corrosion in HCl Solution. *Int J Electrochem Sci* **2020**, *15*, 4739-4753, https://doi.org/10.20964/2020.05.86.
33. Al-Qudah, M. A.; AL-Keifi, H. G.; Al-Momani, I. F.; Abu-Orabi, S. T. Capparis Aegyptia as a green inhibitor for aluminum corrosion in alkaline media. *Int J Corros Scale Inhib* **2021**, *9*, 201-218, https://doi.org/10.17675/2305-6894-2020-9-1-12.
34. Zhu, L.; Zheng, X.; Zeng, X.; Gong, M.; Guo, L. Experimental and theoretical investigation on the effect of N-substituent position on the inhibition performance of l-lysine derivatives for carbon steel in H 2 SO 4 solution. *Res Chem Intermed* **2020**, *47*, 663-682, https://doi.org/10.1007/s11164-020-04292-8.
35. Iroha, N. B.; Maduelosi, N. J. Corrosion inhibitive action and adsorption behaviour of justicia secunda leaves extract as an eco-friendly inhibitor for aluminium in acidic media. *Biointerface Res Appl Chem* **2021**, *11*, 13019-13030, https://doi.org/10.33263/BRIAC115.1301913030.
36. Fernine, Y.; Ech-chihbi, E.; Arrousse, N.; El Hajjaji, F.; Bousraf, F.; Touhami, M. E.; Taleb, M. Ocimum basilicium seeds extract as an environmentally friendly antioxidant and corrosion inhibitor for aluminium alloy 2024-T3 corrosion in 3 wt% NaCl medium. *Colloids Surf A Physicochem Eng Asp* **2021**, *627*, 127232, https://doi.org/10.1016/j.colsurfa.2021.127232.
37. Karki, N.; Neupane, S.; Chaudhary, Y.; Gupta, D. K.; Yadav, A. P. Equisetum hyemale: a new candidate for green corrosion inhibitor family. *Int J Corros Scale Inhib* **2021**, *10*, 206-227, https://doi.org/10.17675/2305-6894-2021-10-1-12.
38. Fernandes, C. M.; Fagundes, T. D. S. F.; dos Santos, N. E.; Rocha, T. S. D. M.; Garrett, R.; Borges, R. M.; Ponzio, E. A. Ircinia strobilina crude extract as corrosion inhibitor for mild steel in acid medium. *Electrochim Acta* **2019**, *312*, 137-148, https://doi.org/10.1016/j.electacta.2019.04.148.

39. Ates, S.; Baran Aydın, E.; Yazıcı, B. The corrosion behavior of the SnO2-coated mild steel in HCl solution at different temperature. *J Adhes Sci Technol* **2021**, *35*, .419-435, https://doi.org/10.1080/01694243.2020.1807240.
40. Haque, J.; Srivastava, V.; Verma, C.; Quraishi, M. A. Experimental and quantum chemical analysis of 2-amino-3-((4-((S)-2-amino-2-carboxyethyl)-1H-imidazol-2-yl) thio) propionic acid as new and green corrosion inhibitor for mild steel in 1 M hydrochloric acid solution. *J Mol Liq* **2017**, *225*, 848-855, https://doi.org/10.1016/j.molliq.2016.11.011.
41. El-Hashemy, M. A.; Sallam, A. The inhibitive action of Calendula officinalis flower heads extract for mild steel corrosion in 1 M HCl solution. *J Mater Res Technol* **2020**, *9*, 13509-13523, https://doi.org/10.1016/j.jmrt.2020.09.078.
42. Chaouiki, A.; Lgaz, H.; Chung, I. M.; Ali, I.H.; Gaonkar, S.L.; Bhat, K.S.; Khan, M. Understanding corrosion inhibition of mild steel in acid medium by new benzonitriles: insights from experimental and computational studies. *J Mol Liq* **2018**, *266*, 603-616, https://doi.org/10.1016/j.molliq.2018.06.103.
43. Guo, W.; Umar, A.; Zhao, Q.; Alsaiari, M. A.; Wang, L.; Pei, M. Corrosion inhibition of carbon steel by three kinds of expired cephalosporins in 0.1 M H_2SO_4. *J Mol Liq* **2020**, *320*, 114295, https://doi.org/10.1016/j.molliq.2020.114295.
44. Baig, N.; Chauhan, D. S.; Saleh, T. A.; Quraishi, M. A. Diethylenetriamine functionalized graphene oxide as a novel corrosion inhibitor for mild steel in hydrochloric acid solutions. *New J Chem* **2019**, *43*, 2328-2337, https://doi.org/10.1039/C8NJ04771E.
45. Gupta, R. K.; Malviya, M.; Ansari, K. R.; Lgaz, H.; Chauhan, D. S.; Quraishi, M. A. Functionalized graphene oxide as a new generation corrosion inhibitor for industrial pickling process: DFT and experimental approach. *Mater Chem Phys* **2019**, *236*, 121727, https://doi.org/10.1016/j.matchemphys.2019.121727.
46. Fatima, S.; Sharma, R.; Asghar, F.; Kamal, A.; Badshah, A.; Kraatz, H. B. Study of new amphiphiles based on ferrocene containing thioureas as efficient corrosion inhibitors: Gravimetric, electrochemical, SEM and DFT studies. *J Ind EngChem* **2019**, *76*, 374-387, https://doi.org/10.1016/j.jiec.2019.04.003.
47. Hynes, N. R. J.; Selvaraj, R. M.; Mohamed, T.; Mukesh, A. M.; Olfa, K.; Nikolova, M. P. Aerva lanata flowers extract as green corrosion inhibitor of low-carbon steel in HCl solution: an in vitro study. *Chem Pap* **2021**, *75*, 1165-1174, https://doi.org/10.1007/s11696-020-01361-5.
48. Farhadian, A.; Rahimi, A.; Safaei, N.; Shaabani, A.; Abdouss, M.; Alavi, A. A theoretical and experimental study of castor oil-based inhibitor for corrosion inhibition of mild steel in acidic medium at elevated temperatures. *Corros Sci* **2020**, *175*, 108871, https://doi.org/10.1016/j.corsci.2020.108871.
49. Fouda, A. S.; Mohamed, O. A.; Elabbasy, H. M. Ferula hermonis Plant Extract as Safe Corrosion Inhibitor for Zinc in Hydrochloric Acid Solution. *J Bio- Tribo-Corros* **2021**, *7*, 1-18, https://doi.org/10.1007/s40735-021-00570-z.
50. Ogunleye, O. O.; Arinkoola, A. O.; Eletta, O. A.; Agbede, O. O.; Osho, Y. A.; Morakinyo, A. F.; Hamed, J. O. Green corrosion inhibition and adsorption characteristics of Luffa cylindrica leaf extract on mild steel in hydrochloric acid environment. *Heliyon* **2020**, *6*, 03205, https://doi.org/10.1016/j.heliyon.2020.e03205.
51. Erami, R. S.; Amirnasr, M.; Meghdadi, S.; Talebian, M.; Farrokhpour, H.; Raeissi, K. Carboxamide derivatives as new corrosion inhibitors for mild steel protection in hydrochloric acid solution. *Corros Sci* **2019**, *151*, 190-197, https://doi.org/10.1016/j.corsci.2019.02.019.
52. Abdel-Gaber, A. M.; Rahal, H. T.; Beqai, F. T. Eucalyptus leaf extract as a eco-friendly corrosion inhibitor for mild steel in sulfuric and phosphoric acid solutions. *Int J Ind Chem* **2020**, 1-10, https://doi.org/10.1007/s40090-020-00207-z.
53. Pavithra, N. S.; Alva, V. D.; Bangera, S. A Sustainable and Green Approach to Corrosion Inhibition of Mild Steel by Rangoon Creeper Flower Extract in 1 M HCl. *Surf Eng Appl Electrochem* **2021** , *57*, 455-465, https://doi.org/10.3103/S106837552104013X.
54. Toghan, A.; Gadow, H. S.; Dardeer, H. M.; Elabbasy, H. M. New promising halogenated cyclic imides derivatives as potential corrosion inhibitors for carbon steel in hydrochloric acid solution. *J Mol Liq* **2021**, *325*, 115136, https://doi.org/10.1016/j.molliq.2020.115136.
55. Ojha, L. K.; Tuzun, B.; Bhawsar, J. Experimental and Theoretical Study of Effect of Allium sativum Extracts as Corrosion Inhibitor on Mild Steel in 1 M HCl Medium. *J Bio- Tribo-Corros* **2020**, *6*, 1-10, https://doi.org/10.1007/s40735-020-00336-z.
56. Rathod, M.; Rajappa, S. K.; Praveen, B. M.; Bharath, D. K. Investigation of Dolichandra unguis-cati leaves extract as a corrosion inhibitor for mild steel in acid medium. *CRGSC* **2021**, *4*, 100113. https://doi.org/10.1016/j.crgsc.2021.100113.

57. Verma, C.; Ebenso, E. E.; Quraishi, M. A. Molecular structural aspects of organic corrosion inhibitors: influence of–CN and–NO2 substituents on designing of potential corrosion: inhibitors for aqueous media. *J Mol Liq* **2020**, *316*, 113874, https://doi.org/10.1016/j.molliq.2020.113874.
58. Kumari, P. P.; Shetty, P.; Rao, S. A.; Sunil, D.; Vishwanath, T. Synthesis, characterization and anti-corrosion behaviour of a novel hydrazide derivative on mild steel in hydrochloric acid medium. *Bull Mater Sci* **2020**, *43*, 1-14, https://doi.org/10.1007/s12034-019-1995-x.
59. Fouda, A. E. A. S.; Abd El-Maksoud, S. A.; El-Sayed, E. H.; Elbaz, H. A.; Abousalem, A. S. Experimental and surface morphological studies of corrosion inhibition on carbon steel in HCl solution using some new hydrazide derivatives. *RSC Advances* **2021**, *11*, 13497-13512, https://doi.org/10.1039/D1RA01405F. .
60. Fouda, A. S.; Motaal, S. M. A.; Ahmed, A. S.; Sallam, H. B.; Ezzat, A.; El-Hossiany, A. Corrosion Protection of Carbon Steel in 2 M HCl Using Aizoon canariense Extract. *Biointerface Res Appl Chem* **2021**, *12*, 230, https://doi.org/10.33263/BRIAC121.230243.
61. Lavanya, D. K.; Priya, F. V.; Vijaya, D. P. Green Approach to Corrosion Inhibition of Mild Steel in Hydrochloric Acid by 1-[Morpholin-4-yl (thiophen-2-yl) methyl] thiourea. *J Fail Anal Prev* **2020**, 494-502, https://doi.org/10.1007/s11668-020-00850-9.
62. Gao, L.; Peng, S.; Huang, X.; Gong, Z. A combined experimental and theoretical study of papain as a biological eco-friendly inhibitor for copper corrosion in H2SO4 medium. *Appl Surf Sci* **2020**, 511, 145446, https://doi.org/10.1016/j.apsusc.2020.145446.
63. Bangera, S.; Alva, V. D. Corrosion Inhibitive Property of Environmentally Benign Syzygium jambos Leaf Extract on Mild Steel in 1 M HCl. *J Fail Anal Prev* **2020**, *20*, 734-743, https://doi.org/10.1007/s11668-020-00869-y.
64. Jafar Mazumder, M. A. New, Amino Acid Based Zwitterionic Polymers as Promising Corrosion Inhibitors of Mild Steel in 1 M HCl. *Coatings* **2019**, *9*, 675, https://doi.org/10.3390/coatings9100675.
65. Kavitha, N.; Ravichandran, J.; Murugesh, A. An Eco-friendly Leucas Aspera Leaves Extract Inhibitor for Copper Corrosion in Hydrochloric Acid Medium. *J Bio- Tribo-Corros* **2020**, *6*, 1-10, https://doi.org/10.1007/s40735-020-00400-8.
66. Meshram, Y. K.; Gunjate, J. K.; Khope, R. U. Studies on adsorption characteristics of manganese onto coal based chemically modified activated carbon. Mater Today: Proc **2020**, *29*, 1185-1191, https://doi.org/10.1016/j.matpr.2020.05.428.
67. Rbaa, M.; Benhiba, F.; Hssisou, R.; Lakhrissi, Y.; Lakhrissi, B.; Touhami, M. E.; Zarrouk, A. Green synthesis of novel carbohydrate polymer chitosan oligosaccharide grafted on d-glucose derivative as bio-based corrosion inhibitor. *J Mol Liq* **2020**, *322*, 114549, https://doi.org/10.1016/j.molliq.2020.114549.
68. Durodola, S. S.; Adekunle, A. S.; Olasunkanmi, L. O.; Oyekunle, J. A. Inhibition of Mild Steel Corrosion in Acidic Medium by Extract of Spilanthes Uliginosa Leaves. *Electroanalysis* **2020**, 1-32, https://doi.org/10.1002/elan.202060227.
69. Saxena, A.; Thakur, K. K.; Bhardwaj, N. Electrochemical studies and surface examination of low carbon steel by applying the extract of Musa acuminata. *Surf Interfaces* **2020**, *18*, 10043,. https://doi.org/10.1016/j.surfin.2020.100436.
70. Fadhil, A. A.; Khadom, A. A.; Ahmed, S. K.; Liu, H.; Fu, C.; Mahood, H. B. Portulaca grandiflora as new green corrosion inhibitor for mild steel protection in hydrochloric acid: Quantitative, electrochemical, surface and spectroscopic investigations. *Surf Interfaces* **2020**, *20*, 100595, https://doi.org/10.1016/j.surfin.2020.100595.
71. Mohd, N. K.; Kian, Y. S.; Ibrahim, N. A.; Nor, S. M. M.; Wan Yunus, W. M. Z.; Ghazali, M. J.; Huei, L. W. Corrosion inhibition, adsorption and thermodynamic properties of hydrophobic-tailed imines on carbon steel in hydrochloric acid solution: a comparative study. *J Adhes Sci Technol* **2021**, 1-22, https://doi.org/10.1080/01694243.2021.1892426.
72. de Sampaio, M. T.; Fernandes, C. M.; de Souza, G. G.; Carvalho, E. S.; Velasco, J. A.; Silva, J. C. M.; Ponzio, E. A. Evaluation of aqueous extract of Mandevilla fragrans leaves as environmental-friendly corrosion inhibitor for mild steel in acid medium. *J Bio- Tribo-Corros* **2021**, *7*, 1-11, https://doi.org/10.1007/s40735-020-00445-9.
73. Amira, W. E.; Rahim, A. A.; Osman, H.; Awang, K.; Raja, P. B. Corrosion inhibition of mild steel in 1 M HCl solution by Xylopia ferruginea leaves from different extract and partitions. *Int. J. Electrochem. Sci* **2011**, *6*, 2998-3016.
74. Ostovari, A.; Hoseinieh, S. M.; Peikari, M.; Shadizadeh, S. R.; Hashemi, S. J. Corrosion inhibition of mild steel in 1 M HCl solution by henna extract: A comparative study of the inhibition by henna and its constituents (Lawsone, Gallic acid, α-d-Glucose and Tannic acid). *Corros Sci* **2009**, *51*, 1935-1949, https://doi.org/10.1016/j.corsci.2009.05.024.

75. Owate, I. O.; Nwadiuko, O. C.; Dike, I. I.; Isu, J. O.; Nnanna, L. A. Inhibition of mild steel corrosion by Aspilia africana in acidic solution. *Am J Mater Sci* **2014**, *4*, 144-149, http://citeseerx.ist.psu.edu/viewdoc/download?doi=10.1.1.1090.7642&rep=rep1&type=pdf.
76. Srivastava, M.; Tiwari, P.; Srivastava, S. K.; Kumar, A.; Ji, G.; Prakash, R. Low cost aqueous extract of Pisum sativum peels for inhibition of mild steel corrosion. *J Mol Liq* **2018**, *254*, 357-368, https://doi.org/10.1016/j.molliq.2018.01.137.